PHYSICAL REVIEW D **93,** 053018 (2016)

Improved effective vector boson approximation revisited

Werner Bernreuther[*] and Long Chen[†]

Institut für Theoretische Teilchenphysik und Kosmologie, RWTH Aachen University, 52056 Aachen, Germany

(Received 27 November 2015; published 30 March 2016)

We reexamine the improved effective vector boson approximation which is based on two-vector-boson luminosities $\mathbf{L}_{\rm pol}$ for the computation of weak gauge-boson hard scattering subprocesses $V_1V_2 \to \mathcal{W}$ in high-energy hadron-hadron or e^-e^+ collisions. We calculate these luminosities for the nine combinations of the transverse and longitudinal polarizations of V_1 and V_2 in the unitary and axial gauge. For these two gauge choices the quality of this approach is investigated for the reactions $e^-e^+ \to W^-W^+\nu_e\bar{\nu}_e$ and $e^-e^+ \to t\bar{t}\nu_e\bar{\nu}_e$ using appropriate phase-space cuts.

DOI: 10.1103/PhysRevD.93.053018

I. INTRODUCTION

Although the discovery of the 125 GeV Higgs boson [1,2] at the Large Hadron Collider strongly supports the Higgs mechanism of electroweak symmetry breaking (EWSB), it does not exclude the possibility that additional (spin-zero) resonances linked to EWSB with masses in or below the TeV range exist. Therefore, the detailed exploration of this issue remains to be one of the prime present and future research goals at this machine and at future high-energy proton-proton or electron-positron colliders that are presently being discussed. One of the most direct probes of the dynamics of EWSB is the high-energy scattering of electroweak gauge bosons $V = W^{\pm}, Z$, especially of longitudinally polarized ones [3–6]. As weak gauge-boson beams are not available, V_1V_2 scattering or fusion can be studied at pp or e^-e^+ colliders only through reactions of the form $f_1f_2 \to f_1'f_2'\mathcal{W}$, where the f_i, f_i' denote quarks (leptons) in the case of pp (e^-e^+) colliders. Typical final states $\mathcal{W}$ of interest are a heavy non-standard Higgs boson, a weak gauge-boson pair $V_1'V_2'$, or a top-quark top antiquark ($t\bar{t}$) pair. At very high energies such reactions, which involve the scattering or fusion of two vector bosons, have often been analyzed by means of the effective vector boson approximation (EVBA) [7–9]. In this approximation the vector boson V radiated off an (anti)quark or electron/positron is treated as a constituent of the respective fermion. In the pioneering works [7–9] the weak gauge boson distribution functions were computed in the leading logarithmic approximation. The QCD radiative corrections to these functions were calculated in [10]. The method was validated in [11] within the axial gauge for the case of heavy Higgs-boson production [11] that is dominated by the fusion of two longitudinally polarized weak gauge bosons, and more recently in [12] using the same gauge. The applicability and limitations of the EVBA in the leading logarithmic approximation and of improved versions [14,15] to heavy fermion production and to $V_1V_2 \to V_1'V_2'$ scattering have been analyzed in many papers, including [11–13,16–24]. To date one may question the need of this approximation, which singles out a certain class of contributions to the complete scattering amplitude, especially in view that powerful computer packages exist, including [25,26] at leading order and [26–28] at next-to-leading order, which allow us to numerically compute the respective processes exactly at the respective order of perturbation theory. Yet, the EVBA may still be useful in appropriate kinematic regions as a tool for analyzing in a transparent way weak gauge-boson reactions that are relevant for the physics of electroweak symmetry breaking; cf. for instance, the recent applications [12,29].

A critical point of the EVBA in the leading logarithmic expansion are the approximations in the computation of the vector-boson distribution functions $F_\lambda(\xi)$. [Here $F_\lambda(\xi)$ has the usual interpretation as the probability of finding a vector boson with helicity λ and longitudinal momentum fraction ξ in an incoming high-energy fermion f.] While the leading logarithmic approximation works reasonably well for a longitudinally polarized vector boson if $\xi > 0.05$ and the center-of-mass energy of the initial state is larger than $\sim$1 TeV, the distribution functions $F_T(\xi)$ for a transversely polarized weak gauge boson computed in the leading logarithmic expansion considerably overestimate the respective exact distribution functions [14]. The distribution functions presented in [14] were calculated without approximations related to kinematics. A further improvement of the EVBA was worked out in [15] for the case of two-vector boson processes, which are the reactions of interest for probing the dynamics of EWSB. Simple convolutions of two single vector boson distribution functions do not account for the mutual influence of the emission of boson V_1 on the probability for the emission of V_2 and vice versa. This is incorporated in the two-vector-boson luminosities derived in [15] in the unitary gauge. Moreover, nondiagonal terms in the summation over the polarizations

[*]breuther@physik.rwth-aachen.de
[†]algeochen@physik.rwth-aachen.de

of V_1 and V_2 were also taken into account in this work, and no kinematic approximations were used. In this approach, a dynamical approximation remains, namely the on-mass-shell continuation of the $V_1V_2 \to \mathcal{W}$ hard scattering cross section. Yet the set of these correlated two-vector boson luminosities is gauge-dependent.

The fact that the subset of diagrams to the reactions $f_1f_2 \to f_1'f_2'\mathcal{W}$ which describe the scattering of two off-shell gauge bosons $V_1V_2 \to \mathcal{W}$ is gauge dependent is another critical point of the (improved) EVBA. It is well-known that in particular in the unitary gauge the off-shell hard scattering subamplitudes show, apart from specific examples, a bad high-energy behavior [13]. It was argued in [11,12] that in the axial gauge and using the EVBA in the leading logarithmic approximation the problem of bad off-shell behavior can be avoided and the effective vector boson approximation works in this gauge if certain (kinematic) conditions are met. In [21] numerical studies of W^+W^- production were performed by computing both the full set of Feynman diagrams and the subset of scattering diagrams associated with $W^+W^- \to W^+W^-$, using the unitary, axial, and a covariant gauge. It was found that when computing the cross section with the scattering diagrams only, the axial gauge (for a specific choice of the associated vector n^μ) yields within these gauge-choices the best approximation to the full, gauge-independent cross section. Applications of the improved EVBA formulation of [15], which uses the dynamical approximation mentioned above (cf. Sec. II), include [21,22,30], with conclusions that are not unanimous. While [21] states that this framework provides not more than a very rough estimate, Ref. [22] and [30] report, for $\mathcal{W} = W^+W^-$ and $\mathcal{W} = ZZ$, an agreement of this approximation with the full result within about 20% to 25% and 10%, respectively.

The effective vector boson approximation in the axial gauge using the EVBA in the leading logarithmic approximation was recently analyzed in detail for single W-boson emission [12]. One may ask whether the improved EVBA setup with correlated two-vector-boson luminosities [15] derived in the axial gauge provides a useful approximation to processes that involve the scattering of two gauge bosons.

In this paper we revisit the approach of [15] which we call here the improved effective vector boson approximation. We reexamine the two-vector-boson luminosities given in [15] in the unitary gauge and clarify an issue related to relative minus signs. As a new aspect we compute the two-vector-boson luminosities which involve a parity-odd combination of the vector and axial vector coupling of V_1 or V_2. They are relevant for processes where the hard-scattering matrix element $V_1(\lambda_1)V_2(\lambda_2) \to \mathcal{W}$ involves parity-violating interactions. This is the case, for instance, for $\mathcal{W} = t\bar{t}$ in the standard model. In addition we compute the two-vector-boson luminosities in the axial gauge. To our knowledge this is a new result. Moreover, we investigate the quality of the improved EVBA in both gauges for two examples. To be specific we consider high-energy e^-e^+ collisions and analyze the processes $e^-e^+ \to W^-W^+\nu_e\bar{\nu}_e$ and $e^-e^+ \to t\bar{t}\nu_e\bar{\nu}_e$ to lowest order in the standard model. We compute the respective tree-level cross sections both within the improved EVBA and fully with the computer code MadGraph [26], i.e., taking into account all contributing Feynman diagrams, and compare the relative differences using appropriate cuts on the final-state particles.

The paper is organized as follows. In Sec. II we outline the approach of Kuss and Spiesberger (KS) [15] in deriving improved two-vector-boson luminosities. We clarify an issue related to relative minus signs and we compute luminosities which involve parity-even and parity-odd combinations of the vector and axial vector coupling of V_1 or V_2. The formulas apply to both incoming quarks and leptons. For W^-W^+ bosons radiated off e^-e^+, we compare our results for the "parity-even" luminosities with those of [15]. In Sec. III we compute the two-vector-boson luminosities in the axial gauge. Section IV contains our comparison of the cross sections for $e^-e^+ \to W^-W^+\nu_e\bar{\nu}_e$ and $e^-e^+ \to t\bar{t}\nu_e\bar{\nu}_e$ computed exactly and with the improved EVBA. We conclude in Sec. V. Appendixes A and B contain our results for the four-fold differential luminosities in the unitary and axial gauge.

II. THE KS LUMINOSITY FORMULA

We consider the production of an arbitrary state $\mathcal{W}$ by the scattering of two light fermions:

$$f_1(l_1) + f_2(l_2) \to f_1'(l_1') + f_2'(l_2') + \mathcal{W}(p_\mathcal{W}), \quad (1)$$

where f_i (f_i') denote the fermions in the initial (final) state and the symbols in brackets are the associated four-momenta. The cross section of this process is given by

$$\sigma_{f_1f_2} = \frac{1}{2s}\int \mathrm{d}\Gamma_2 \mathrm{d}\tilde{p}_\mathcal{W}\delta^{(4)}(l_1 + l_2 - l_1' - l_2' - p_\mathcal{W}) \times \overline{|\mathcal{M}_{f_1f_2\to f_1'f_2'\mathcal{W}}|^2}, \quad (2)$$

where $s = (l_1 + l_2)^2$, $\mathrm{d}\Gamma_2 \equiv \mathrm{d}^3\vec{l}_1'\mathrm{d}^3\vec{l}_2'/(16\pi^2E_1'E_2')$, and $\mathrm{d}\tilde{p}_\mathcal{W} \equiv \mathrm{d}^3p_\mathcal{W}/[(2\pi)^3 2E_\mathcal{W}]$. Moreover, $\overline{|\mathcal{M}|^2}$ denotes the squared matrix element of (1) which is averaged and summed over the helicities (and colors, in the case of quarks) of the fermions f_i and f_i', respectively.

In the following we consider processes (1) which proceed via the exchange of two off-shell weak gauge bosons V_1, V_2 ($V = W, Z$) with masses m_1, m_2, as depicted in Fig. 1.

In the unitary gauge, which was used in [15], the matrix element which corresponds to the diagram Fig. 1 takes the form

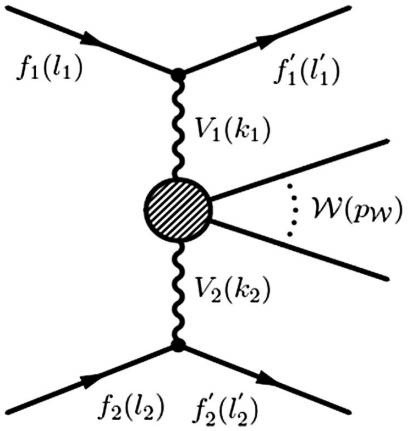

FIG. 1. Generic weak gauge-boson scattering diagram.

$$\mathcal{M}_{f_1f_2\to f_1'f_2'\mathcal{W}} = j_{1\mu}(l_1,l_1')\frac{iP^{\mu\mu'}(k_1)}{k_1^2-m_1^2} \times j_{2\nu}(l_2,l_2')\frac{iP^{\nu\nu'}(k_2)}{k_2^2-m_2^2}\mathcal{M}^{\mathcal{W}}_{\mu'\nu'}, \quad (3)$$

where $k_i = l_i - l_i'$ ($k_i^2 \le 0$) and $P^{\alpha\beta}(k) = -g^{\alpha\beta} + k^\alpha k^\beta/m_V^2$ for massive gauge-bosons in the unitary gauge. The four-vectors j_1^μ, j_2^ν denote the charged or neutral fermion currents and $\mathcal{M}^{\mathcal{W}}_{\mu'\nu'}$ is the vector-boson fusion amplitude for the process $V_1V_2 \to \mathcal{W}$ that must be evaluated for off-shell gauge bosons.

Depending on whether the pairs f_1, f_1' and f_2, f_2' are particles or antiparticles, the current j_1^μ or j_2^ν is either composed of u or v Dirac spinors:

$$e\overline{u}_{f'}(l')(a\gamma^\mu + b\gamma^\mu\gamma_5)u_f(l) \quad \text{or}$$
$$e\overline{v}_f(l)(a\gamma^\mu + b\gamma^\mu\gamma_5)v_{f'}(l'), \quad (4)$$

where e denotes the positron charge. We are interested in the processes (1) at high energies where the masses of the light fermions f_i, f_i' can be safely neglected, i.e., where $k_i^\mu j_{i\mu} = 0$ ($i = 1, 2$) holds to very good approximation. In order to decompose $g^{\mu\nu}$ we introduce two sets of polarization vectors $\varepsilon_j^\mu(\lambda)$ ($j = 1, 2$) that are mutually orthogonal and orthogonal to k_j^μ and obey the normalization convention

$$\varepsilon_j(\lambda)\cdot\varepsilon_j^*(\lambda') = (-1)^\lambda\delta_{\lambda,\lambda'}, \qquad j = 1,2, \quad \lambda = 0,\pm1. \quad (5)$$

An explicit representation of $\varepsilon_j^\mu(\lambda)$ in the center-of-mass frame of V_1 and V_2 is given in Appendix A. With these polarization vectors one obtains

$$-g^{\mu\nu} = -\frac{k_j^\mu k_j^\nu}{k_j^2} + \sum_{\lambda=\pm1,0}(-1)^{\lambda+1}\varepsilon_j^{*\mu}(\lambda)\varepsilon_j^\nu(\lambda), \quad j = 1,2 \quad (6)$$

which holds for any spacelike four-momentum k_j^μ.

With (6) one can rewrite (3):

$$\mathcal{M}_{f_1f_2\to f_1'f_2'\mathcal{W}} = i^2\sum_{\lambda_1,\lambda_2}(-1)^{\lambda_1+\lambda_2}\frac{j_1(l_1,l_1')\cdot\varepsilon_1^*(\lambda_1)}{k_1^2-m_1^2} \times\frac{j_2(l_2,l_2')\cdot\varepsilon_2^*(\lambda_2)}{k_2^2-m_2^2}\mathcal{M}^{\mathcal{W}}_{\lambda_1\lambda_2}, \quad (7)$$

where the labels λ_1, λ_2 take the values $0, \pm1$ and $\mathcal{M}^{\mathcal{W}}_{\lambda_1\lambda_2} \equiv \varepsilon_1^\mu(\lambda_1)\varepsilon_2^\nu(\lambda_2)\mathcal{M}^{\mathcal{W}}_{\mu,\nu}$.

Squaring (7) and averaging and summing over the spins (and colors, in the case of quarks) of the initial-state and final-state fermions f_i, f_i', one gets

$$\overline{|\mathcal{M}_{f_1f_2\to f_1'f_2'\mathcal{W}}|^2} = 4\sum_{\lambda_1,\lambda_1',\lambda_2,\lambda_2'}(-1)^{\lambda_1+\lambda_2+\lambda_1'+\lambda_2'}\frac{T_1(\lambda_1,\lambda_1')}{(k_1^2-m_1^2)^2} \times\frac{T_2(\lambda_2,\lambda_2')}{(k_2^2-m_2^2)^2}\mathcal{M}^{\mathcal{W}}_{\lambda_1\lambda_2}\mathcal{M}^{\mathcal{W}*}_{\lambda_1'\lambda_2'} \quad (8)$$

with

$$T_i(\lambda_i,\lambda_i') = \frac{1}{4}\sum j_i(l_i,l_i')\cdot\varepsilon_i^*(\lambda_i)j_i^*(l_i,l_i')\cdot\varepsilon_i(\lambda_i'), \quad (9)$$

and the sum in (9) refers to fermion-spin summation.

In [15] both the diagonal ($\lambda_i = \lambda_i'$) and nondiagonal ($\lambda_i \ne \lambda_i'$) components of the helicity tensors (9) were taken into account in the computation of the vector boson luminosities. The results of [15] derived in the unitary gauge show that the nondiagonal vector-boson luminosities are (significantly) smaller than the diagonal ones if $0.2 \lesssim x < 1$, where

$$x = \frac{(k_1+k_2)^2}{s} \equiv \frac{\hat{s}}{s}. \quad (10)$$

We consider in the following only the diagonal components of (9) because (i) the domain of applicability of the vector boson approximation is the region where x is not very small and (ii) because of the following conceptual issue. This approach loses its simplicity and appeal if the nondiagonal components are taken into account. Then the resulting cross section can no longer be represented as in Eq. (23) below as a sum of products of two-vector-boson luminosities times the respective hard scattering V_1V_2 cross sections.

In order to simplify the notation we use $T_i(\lambda_i) \equiv e^{-2}T_i(\lambda_i,\lambda_i)$ from now on. Furthermore, we define

$$\tilde{\sigma}(\hat{s},k_1^2,k_2^2;\lambda_1,\lambda_2) \equiv \frac{1}{2\kappa_0}\int d\tilde{p}_\mathcal{W}(2\pi)^4\delta^{(4)}(k_1+k_2-p_\mathcal{W})|\mathcal{M}^{\mathcal{W}}_{\lambda_1\lambda_2}|^2, \quad (11)$$

where

$$\kappa_0 = \sqrt{\hat{s}^2 + m_1^4 + m_2^4 - 2\hat{s}m_1^2 - 2\hat{s}m_2^2 - 2m_1^2m_2^2} \quad (12)$$

and $\hat{s}$ is the squared invariant mass of the intermediate gauge-boson pair defined in (10). Equation (11) may be interpreted as the cross section for off-shell gauge-boson fusion $V_1V_2 \to \mathcal{W}$, where the on-shell flux factor κ_0 is introduced by convention and for later convenience. Using (8), keeping only the diagonal contributions, and using the definition (11), Eq. (2) becomes

$$\sigma_{f_1f_2\to f_1'f_2'\mathcal{W}} = \left(\frac{\alpha}{\pi}\right)^2 \frac{4\kappa_0}{s} \int \mathrm{d}\Gamma_2 \sum_{\lambda_1,\lambda_2} \frac{1}{(k_1^2 - m_1^2)^2} \frac{1}{(k_2^2 - m_2^2)^2} \times \mathcal{L}_{\lambda_1\lambda_2} \tilde{\sigma}(\lambda_1, \lambda_2), \quad (13)$$

where $\alpha = e^2/(4\pi)$ denotes the electromagnetic fine structure constant and

$$\mathcal{L}_{\lambda_1\lambda_2} = T_1(\lambda_1)T_2(\lambda_2). \quad (14)$$

The helicity tensors T_i defined in (9), which are needed for computing the quantities $\mathcal{L}_{\lambda_1\lambda_2}$, can be decomposed as follows:

$$T_i(\lambda_i) = (v_i^2 + a_i^2)\mathcal{C}_i(\lambda_i) + 2v_ia_i\mathcal{S}_i(\lambda_i), \quad i = 1, 2, \quad (15)$$

where

$$\mathcal{C}_j(\lambda_j) = (l_j^\mu l_j'^\nu + l_j'^\mu l_j^\nu - l_j \cdot l_j' g^{\mu\nu})\varepsilon_{j\mu}^*(\lambda_j)\varepsilon_{j\nu}(\lambda_j),$$
$$\mathcal{S}_j(\lambda_j) = -i(-1)^{r_j}\epsilon_{\mu\nu\rho\sigma} l_j'^\mu \varepsilon_j^{*\nu}(\lambda_j) l_j^\rho \varepsilon_j^\sigma(\lambda_j), \quad j = 1, 2. \quad (16)$$

Here we use the convention $\epsilon_{0123} = -1$ and v_i, a_i are the vector and axial vector couplings of the gauge boson V_i in the parametrizations (4) of the currents. For charged currents in the standard model they are given by $v_i = -a_i = 1/(2\sqrt{2}\sin\theta_W)$, times the Cabibbo-Kobayashi-Maskawa mixing matrix element $V_{qq'}$ in the case of quarks. The neutral current couplings are $v_i = (T_3^{f_i} - 2\sin^2\theta_W)/(2\sin\theta_W\cos\theta_W)$ and $a_i = -T_3^{f_i}/(2\sin\theta_W\cos\theta_W)$.

In Eq. (16) the power $r_j = 0$ ($r_j = 1$) if the label $j = 1$, 2 refers to a particle (antiparticle) pair f_j, f_j', i.e., the sign factor depends on whether the fermionic currents (4) involve u- or v-spinors.

Rather than working with the nine quantities $\mathcal{L}_{\lambda_1\lambda_2}$, it is convenient to use in (13) the following linear combinations:

$$\begin{aligned}
\mathcal{L}_{\mathrm{TT}} &\equiv \mathcal{L}_{++} + \mathcal{L}_{+-} + \mathcal{L}_{-+} + \mathcal{L}_{--} \\
&= 4(v_1^2 + a_1^2)(v_2^2 + a_2^2)\mathcal{C}_1(+)\mathcal{C}_2(+), \\
\mathcal{L}_{\mathrm{T}\overline{\mathrm{T}}} &\equiv \mathcal{L}_{++} - \mathcal{L}_{+-} + \mathcal{L}_{-+} - \mathcal{L}_{--} \\
&= 8(v_1^2 + a_1^2)(v_2a_2)\mathcal{C}_1(+)\mathcal{S}_2(+), \\
\mathcal{L}_{\overline{\mathrm{T}}\mathrm{T}} &\equiv \mathcal{L}_{++} + \mathcal{L}_{+-} - \mathcal{L}_{-+} - \mathcal{L}_{--} \\
&= 8(v_1a_1)(v_2^2 + a_2^2)\mathcal{S}_1(+)\mathcal{C}_2(+), \\
\mathcal{L}_{\overline{\mathrm{T}}\overline{\mathrm{T}}} &\equiv \mathcal{L}_{++} - \mathcal{L}_{+-} - \mathcal{L}_{-+} + \mathcal{L}_{--} \\
&= 16(v_1a_1)(v_2a_2)\mathcal{S}_1(+)\mathcal{S}_2(+), \\
\mathcal{L}_{\mathrm{TL}} &\equiv \mathcal{L}_{+0} + \mathcal{L}_{-0} = 2(v_1^2 + a_1^2)(v_2^2 + a_2^2)\mathcal{C}_1(+)\mathcal{C}_2(0), \\
\mathcal{L}_{\mathrm{LT}} &\equiv \mathcal{L}_{0+} + \mathcal{L}_{0-} = 2(v_1^2 + a_1^2)(v_2^2 + a_2^2)\mathcal{C}_1(0)\mathcal{C}_2(+), \\
\mathcal{L}_{\overline{\mathrm{T}}\mathrm{L}} &\equiv \mathcal{L}_{+0} - \mathcal{L}_{-0} = 4(v_1a_1)(v_2^2 + a_2^2)\mathcal{S}_1(+)\mathcal{C}_2(0), \\
\mathcal{L}_{\mathrm{L}\overline{\mathrm{T}}} &\equiv \mathcal{L}_{0+} - \mathcal{L}_{0-} = 4(v_1^2 + a_1^2)(v_2a_2)\mathcal{C}_1(0)\mathcal{S}_2(+), \\
\mathcal{L}_{\mathrm{LL}} &\equiv \mathcal{L}_{00} = (v_1^2 + a_1^2)(v_2^2 + a_2^2)\mathcal{C}_1(0)\mathcal{C}_2(0). \quad (17)
\end{aligned}$$

The $V_1V_2 \to \mathcal{W}$ cross sections $\tilde{\sigma}(\lambda_1, \lambda_2)$ in (13) have to be transformed accordingly. One gets nine linear combinations in analogy to (17), but for each index T or $\overline{\mathrm{T}}$ an overall factor $1/2$ is present. Thus, for instance,

$$\begin{aligned}
\tilde{\sigma}_{\mathrm{TT}} &= \frac{1}{4}[\tilde{\sigma}(+,+) + \tilde{\sigma}(+,-) + \tilde{\sigma}(-,+) + \tilde{\sigma}(-,-)], \\
\tilde{\sigma}_{\overline{\mathrm{T}}\mathrm{L}} &= \frac{1}{2}[\tilde{\sigma}(+,0) - \tilde{\sigma}(-,0)], \qquad \tilde{\sigma}_{\mathrm{LL}} = \tilde{\sigma}(0,0), \quad (18)
\end{aligned}$$

etc. Then (13) takes the form

$$\sigma_{f_1f_2\to f_1'f_2'\mathcal{W}} = \left(\frac{\alpha}{\pi}\right)^2 \frac{4\kappa_0}{s} \int \mathrm{d}\Gamma_2 \sum_{\mathrm{pol}} \frac{1}{(k_1^2 - m_1^2)^2} \frac{1}{(k_2^2 - m_2^2)^2} \times \mathcal{L}_{\mathrm{pol}} \tilde{\sigma}_{\mathrm{pol}}, \quad (19)$$

where "pol" labels the nine polarization indices as in (17); i.e., pol = TT, T$\overline{\mathrm{T}}$, etc.

A basic issue of the effective vector boson method is the modeling of the dependence of the off-shell cross section $\tilde{\sigma}_{\mathrm{pol}}(\hat{s}, k_1^2, k_2^2)$ on k_i^2. If both V_1 and V_2 are transversely polarized, it turns out that $\tilde{\sigma}_{\mathrm{pol}}$ is only slowly varying with k_i^2. Thus, one can put $\tilde{\sigma}_{\mathrm{TT}}(\hat{s}, k_1^2, k_2^2) \simeq \tilde{\sigma}_{\mathrm{TT}}(\hat{s}, m_1^2, m_2^2)$ to good approximation. If longitudinal polarizations are involved, $\tilde{\sigma}_{\mathrm{pol}}(\hat{s}, k_1^2, k_2^2)$ contains in the unitary gauge kinematic singularities at $k_i^2 = 0$ which result from the longitudinal polarization vectors $\varepsilon_i^\mu(0)$. The dependence on k_i^2 of $\varepsilon_i^\mu(0)$ [see (A2), (A3)] suggests the following extrapolation [15] of the on-shell $V_1V_2 \to \mathcal{W}$ cross sections to off-shell values of k_i^2:

$$\tilde{\sigma}_{\mathrm{pol}}(\hat{s}, k_1^2, k_2^2) \approx f_{\mathrm{pol}}(k_1^2, k_2^2)\hat{\sigma}_{\mathrm{pol}}(\hat{s}, m_1^2, m_2^2), \quad (20)$$

where $\hat{\sigma}_{\rm pol}$ is the on-shell $V_1V_2 \to \mathcal{W}$ cross section and

$$f_{\rm TT} = f_{\rm T\overline{T}} = f_{\overline{\rm T}\rm T} = f_{\overline{\rm T}\overline{\rm T}} = 1,$$
$$f_{\rm TL} = f_{\overline{\rm T}\rm L} = \frac{m_2^2}{-k_2^2}, \quad f_{\rm LT} = f_{\rm L\overline{T}} = \frac{m_1^2}{-k_1^2}, \quad f_{\rm LL} = \frac{m_1^2 m_2^2}{k_1^2 k_2^2}. \tag{21}$$

The quantities $\mathcal{L}_{\rm pol}$ defined in (17) are computed using (14)–(16). Because the helicities of a massive particle are dependent on the Lorentz frame, we define the associated polarization vectors in the center-of-mass frame of V_1 and V_2, as already mentioned above. They are given in Eqs. (A2), (A3) of Appendix A. The Minkowski scalar products which appear in the expressions for the form factors C_1, S_1 (C_2, S_2) are conveniently evaluated in a Breit frame B_1 (B_2) which is defined such that only the z component of the four-momentum k_1^μ (k_2^μ) is nonvanishing in B_1 (B_2). The polarization vectors of V_1 (V_2) defined in the V_1V_2 center-of-mass frame must be Lorentz-transformed to B_1 (B_2). The resulting polarization vectors and four-momenta of V_1 (V_2) in B_1 (B_2) are given in [15]. We have computed the form factors $C_{1,2}$ and $S_{1,2}$ using these parametrizations. Our results agree with those given in Appendix B[1] of [15], up to an overall sign factor $(-1)^{r_j}$ associated with S_i. This factor appears if the form factor S_i is defined according to Eq. (16).

It is appropriate to rewrite the phase-space integral in (19) in terms of new variables. One uses that $k_{1,2}^2 < 0$ in the physical region. Moreover, one uses (10) and

$$u = 2k_1 \cdot l_2 + l_2^2 = 2k_1 \cdot l_2, \tag{22}$$

and the azimuthal angle ϕ_1 (ϕ_2) of the final-state fermion f_1' (f_2') in the Breit system B_1 (B_2). With (20) the cross section (19) in the improved effective vector boson approximation (IEVBA) in the unitary gauge takes the form

$$\sigma^{\rm IEVBA}_{f_1f_2\to f_1'f_2'\mathcal{W}} = \sum_{\rm pol} \int_{x_{\rm min}}^1 {\rm d}x \mathbf{L}_{\rm pol}(x) \hat{\sigma}_{\rm pol}(\hat{s} = xs, m_1^2, m_2^2), \tag{23}$$

where

$$\mathbf{L}_{\rm pol}(x) \equiv \left(\frac{\alpha}{2\pi}\right)^2 \frac{\kappa_0}{s} \int_{-s+\hat{s}}^0 {\rm d}k_1^2 \int_{-s+\hat{s}'}^0 {\rm d}k_2^2 \int_{\hat{x}s}^s \frac{{\rm d}u}{u} \times \frac{k_1^2}{(k_1^2 - m_1^2)^2} \frac{k_2^2}{(k_2^2 - m_2^2)^2} f_{\rm pol} \mathcal{J}_{\rm pol} \tag{24}$$

and

$$\mathcal{J}_{\rm pol} \equiv \frac{1}{k_1^2 k_2^2} \int_0^{2\pi} \frac{{\rm d}\phi_1}{2\pi} \int_0^{2\pi} \frac{{\rm d}\phi_2}{2\pi} \mathcal{L}_{\rm pol}. \tag{25}$$

The integration boundaries in (23) and (24) are as follows: $x_{\rm min} = \hat{s}_{\rm min}/s$, where $\hat{s}_{\rm min} = p_{\mathcal{W},\rm min}^2$ is the minimal value of $\hat{s}$ for the production of the final state $\mathcal{W}$. The variables $\hat{s}'$ and $\hat{x}$ which appear in the boundaries of the integrals in (24) are given by

$$\hat{s}' = \frac{s}{s + k_1^2} \hat{s}, \qquad \hat{x} = \frac{1}{s}\left(\nu + \frac{1}{2}\kappa\right), \tag{26}$$

where

$$\nu = k_1 \cdot k_2 = \frac{1}{2}(\hat{s} - k_1^2 - k_2^2), \quad \kappa = 2\sqrt{\nu^2 - k_1^2 k_2^2}. \tag{27}$$

The dimensionless functions $\mathbf{L}_{\rm pol}(x)$ are the vector-boson pair luminosities of V_1 and V_2. The product $\mathbf{L}_{\rm pol}(x)dx$ can be interpreted as the probability for emitting from f_1 and f_2 the vector bosons V_1 and V_2 with specified polarizations and with squared V_1V_2 center-of-mass energy in the interval $[xs, (x + dx)s]$. The nine functions $\mathcal{J}_{\rm pol}$ that depend, for fixed f_1f_2 center-of-mass energy $\sqrt{s}$, on the four variables k_1^2, k_2^2, x and u, are called differential luminosities. Our results for these functions are given in Appendix A.

Integrating the $\mathcal{J}_{\rm pol}$ given in Appendix A with respect to u (which can be done analytically), with the boundaries as in (24), we obtain three-fold differential luminosities. For pol = TT, LT, TL, LL, $\overline{\rm TT}$ these three-fold differential luminosities were calculated before in [15]. We agree with the results[2] of [15] for pol = TT, LT, TL, LL, up to different normalization conventions used. The differential luminosity $\mathcal{J}_{\overline{\rm TT}}$ originates from the product $\mathcal{S}_1(+)\mathcal{S}_2(+)$ as Eq. (17) shows. If the fermion line f_1, $f_1{}'$ in Fig. 1 refers to particles and f_2, $f_2{}'$ to antiparticles or vice versa, this product gets an overall factor (-1) as explained below Eq. (16). This distinction is not made in [15] in the corresponding expression for $\mathcal{J}_{\overline{\rm T}\overline{\rm T}}$.

Our results for pol = $\overline{\rm TT}$, $\rm T\overline{T}$, $\rm L\overline{T}$, and $\overline{\rm T}\rm L$ are not given in [15]. As mentioned in the introduction these luminosities are required if the matrix element $V_1(\lambda_1)V_2(\lambda_2) \to \mathcal{W}$ receives also contributions from parity-violating interactions, cf. Sec. IV.

If one applies cuts on the rapidities of the particles in the final state then the integration range of u is affected. Details are given in Appendix A. Thus in applications it is adequate to perform this integration numerically, see Sec. IV.

The differential luminosities $\mathcal{J}_{\rm pol}$ given in Appendix A and the formulas (23) and (24) apply to both quarks and leptons in the initial state. In Figs. 2 and 3 we show the luminosities $\mathbf{L}_{\rm pol}(x)$ of finding a W^-W^+ pair in unpolarized e^-e^+ at $\sqrt{s} = 2$ TeV. For the computations of these

[1]The formula for $C_1(00)$ given in Appendix B of [15] contains a misprint. The sign in front of the third term in the square bracket should be positive.

[2]The formula for J_{TL} in Eq. 40 of [15] contains a misprint: the first term in the square bracket of the second line should read $3s^2\nu$.

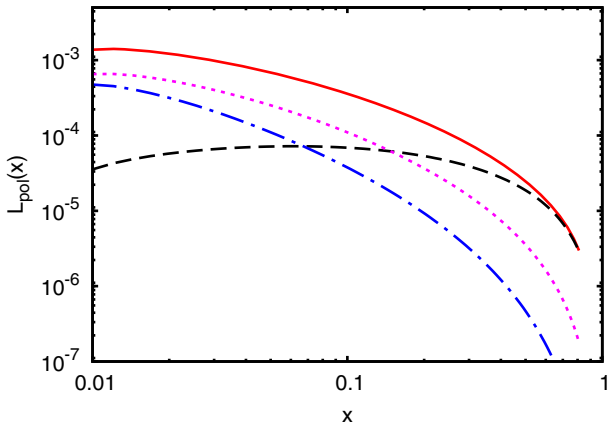

FIG. 2. The luminosities $\mathbf{L}_{\mathrm{TT}}(x)$ (solid red), $\mathbf{L}_{\mathrm{LT}}(x)$ (dotted magenta), $\mathbf{L}_{\mathrm{LL}}(x)$ (dot-dashed blue), and $(-1)\mathbf{L}_{\overline{\mathrm{TT}}}(x)$ (dashed black) in the unitary gauge for a W^-W^+ pair in e^-e^+ collisions at $\sqrt{s} = 2$ TeV.

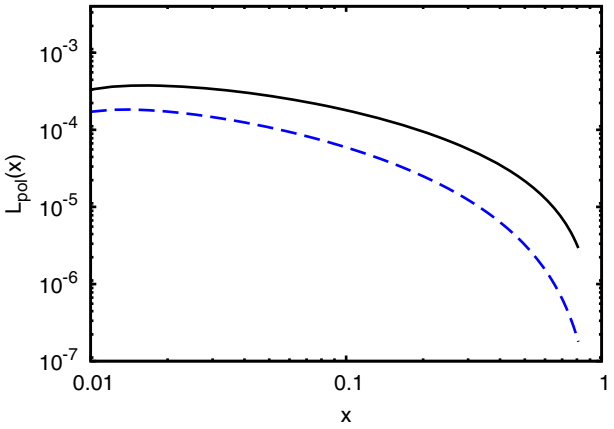

FIG. 3. The luminosities $\mathbf{L}_{\mathrm{T}\overline{\mathrm{T}}}(x)$ (solid black) and $\mathbf{L}_{\mathrm{L}\overline{\mathrm{T}}}(x)$ (dashed blue) in the unitary gauge for a W^-W^+ pair in e^-e^+ collisions at $\sqrt{s} = 2$ TeV.

luminosities we used $\alpha = 1/137.035$, $m_W = 80.385$ GeV $m_Z = 91.1876$ GeV and $\cos\theta_W = m_W/m_Z$. Figure 2 shows the cases pol = TT, LT, LL, and $\overline{\mathrm{TT}}$. CP invariance implies that the luminosity $\mathbf{L}_{\mathrm{TL}} = \mathbf{L}_{\mathrm{LT}}$. The luminosities for pol = TT, LT, LL agree with those displayed in Fig. 2 of [15]. Our luminosity for pol = $\overline{\mathrm{TT}}$, which is negative, differs from the corresponding one given in [15] by an overall minus sign. This sign is convention-independent. The sign difference can be traced back to Eq. (16). The form factor $\mathcal{S}_2(+)$ has a relative minus sign compared with $\mathcal{S}_1(+)$ because the incoming fermion $f_2 = e^+$ is the antiparticle of f_1.

Figure 2 shows that the luminosity $\mathbf{L}_{\mathrm{TT}}$ for transversely polarized W pairs is the largest one. Needless to say, this does not imply that the contributions to (23) from transversely polarized W bosons are always the dominant ones.

Figure 3 shows the luminosities for pol = $\mathrm{T}\overline{\mathrm{T}}, \mathrm{L}\overline{\mathrm{T}}$ that involve parity-odd combinations of vector and axial vector couplings. The first (second) polarization index refers to the polarization of W^- (W^+) radiated from e^- (e^+). These luminosities were not given in [15]. For the example considered here, that is, $e^\mp \to W^\mp\nu_e/\overline{\nu}_e$, and for the case $q \to W^-q'$ and $\overline{q} \to W^+\overline{q}'$, CP invariance implies that

$$\mathbf{L}_{\overline{\mathrm{T}}\mathrm{T}}(x) = -\mathbf{L}_{\mathrm{T}\overline{\mathrm{T}}}(x), \qquad \mathbf{L}_{\overline{\mathrm{T}}\mathrm{L}}(x) = -\mathbf{L}_{\mathrm{L}\overline{\mathrm{T}}}(x). \tag{28}$$

Relations between differential luminosities integrated with respect to u are given, for a general reaction (1), in Eq. (A14) of Appendix A.

If V_1 and/or V_2 is a Z boson, the corresponding luminosities can be obtained in analogous fashion by changing the value of the vector-boson mass m_1 and/or m_2, using the vector and axial-vector neutral current couplings given below (A13), and by integrating $\mathcal{J}_{\mathrm{pol}}$. The V_1V_2 luminosities for vector bosons radiated off quarks are computed analogously.

The above two-boson luminosities do not factorize into single boson distributions, because in the above formulation, the emission of a gauge boson V_1 with definite helicity (defined in the V_1V_2 center-of-mass frame) from f_1 does depend on the squared off-shell mass k_2^2 of V_2, and vice versa. At high energies it seems justified to neglect this mutual dependence on k_i^2, because the fusion process is dominated by small momentum transfers. Neglecting the dependence of the form factors C_1, S_1 (C_2, S_2) on k_2^2 (k_1^2) one obtains a luminosity formula $\mathbf{L}_{\mathrm{pol}}^{\mathrm{conv}}(x)$ which can be represented as a convolution of single vector boson distributions. These single V distributions were first derived in [14]. A further approximation, the so-called leading logarithmic approximation [7–9] (LLA), yields simplified expressions which have often been used in the literature. Here one performs the integral $\int \mathcal{J}_{\mathrm{pol}} du/u$ in (24) analytically. One neglects in the resulting expression the dependence on the k_i^2, performs the high-energy limit $s \ll m_i^2$, and keeps only the leading logarithmic terms.

In this way, $\mathbf{L}_{\mathrm{pol}} \to \mathbf{L}_{\mathrm{pol}}^{\mathrm{LLA}}$. These two approximations were analyzed in detail in [15]. It was also shown by these authors that the ratios $\mathbf{L}_{\mathrm{pol}}^{\mathrm{conv}}/\mathbf{L}_{\mathrm{pol}}$ are significantly larger than one for almost all values of x; only for x close to one, these ratios are also close to one. Moreover, the ratio $\mathbf{L}_{\mathrm{pol}}^{\mathrm{LLA}}/\mathbf{L}_{\mathrm{pol}}$ is even larger. For $x \to 1$ this ratio is approximately close to one only for pol = LL.

III. THE VECTOR-BOSON PAIR LUMINOSITY IN THE AXIAL GAUGE

In this section we derive the vector-boson pair luminosity in the axial gauge

Let us first recapitulate the salient features of the electroweak standard model in the axial gauge. The gauge-fixing term is chosen to be

$$\mathcal{L}_{gf} = -\frac{\xi}{2}[(n\cdot A^a)^2 + (n\cdot B)^2], \tag{29}$$

where A^a_μ and B_μ denote the $\mathrm{SU}(2)_L$ und $\mathrm{U}(1)_Y$ gauge fields and n^μ is a constant vector. As is well-known ghost fields are absent in this gauge, but the Goldstone fields are still present. We parametrize the SM Higgs doublet field by $\Phi = (\phi_W, (v + H + i\phi_Z)/\sqrt{2})$, where H is the physical Higgs field. The part of the Lagrangian bilinear in the gauge and Goldstone fields contains terms that mix these fields. In order to proceed one may either use propagators that are nondiagonal in the gauge-fields (cf. [11]), or one diagonalizes these bilinear terms by appropriate shifts of the Goldstone fields, as was done in [31]. As a consequence, the gauge and Goldstone fields decouple in the propagators, but the Feynman rules for the interactions vertices, given also in [31], become more complicated than those in the covariant renormalizable gauges. We use the approach of [31]. In this framework, the W boson propagator is given in the limit $\xi \to \infty$ by

$$iD^W_{\mu\nu}(k) = \frac{iN_{\mu\nu}}{k^2 - m_W^2 + i\epsilon},$$
$$N_{\mu\nu}(k) = \left(-g_{\mu\nu} + \frac{n_\mu k_\nu + n_\nu k_\mu}{n\cdot k} - k_\mu k_\nu \frac{n^2}{(n\cdot k)^2}\right). \tag{30}$$

The Z-boson (photon) propagator is obtained from (30) by the replacement $m_W^2 \to m_Z^2$ $(m_W^2 \to 0)$.

Because $N^{\mu\nu}n_\nu = 0$ the symmetric propagator matrix $N^{\mu\nu}(k)$ has rank 3. Thus its spectral decomposition can be made in terms of three mutually orthogonal four-vectors $\varepsilon^\mu(\lambda)$, $\lambda = \pm 1, 0$. We obtain, for any spacelike four-momentum k^μ:

$$N^{\mu\nu}(k) = \sum_{\lambda=\pm1} \varepsilon^{*\mu}(\lambda)\varepsilon^\nu(\lambda) - \varepsilon^\mu(0)\varepsilon^\nu(0), \tag{31}$$

where the dependence of the ε^μ on k is not exhibited. The vectors that describe transverse polarization have to satisfy

$$k_\mu\varepsilon^\mu = n_\mu\varepsilon^\mu = 0, \qquad \varepsilon(\lambda)\cdot\varepsilon^*(\lambda') = \delta_{\lambda,\lambda'}, \qquad \lambda,\lambda' = \pm 1.$$

Furthermore we get

$$\varepsilon^\mu(0) = \sqrt{\frac{-k^2}{(k\cdot n)^2 - n^2k^2}}\left(n^\mu - \frac{n^2}{(k\cdot n)}k^\mu\right). \tag{32}$$

In the axial gauge the weak gauge-boson scattering amplitude depicted in Fig. 1 is supplemented by diagrams where one or both of the propagators of the weak gauge bosons V_1, V_2 are replaced by the propagators of the Goldstone bosons ϕ_W, ϕ_Z. However, because the couplings of ϕ_W, ϕ_Z to the fermions f_i, f_i' $(i = 1, 2)$ are proportional to the fermion masses, these contributions vanish in the limit $m_i, m_i' \to 0$, which we consider. Therefore, the scattering amplitude analogous to (3) is given by

$$\mathcal{M}^{\mathrm{axial}}_{f_1f_2\to f_1'f_2'\mathcal{W}} = j_{1\mu}(l_1, l_1')\frac{iN^{\mu\mu'}(k_1)}{k_1^2 - m_1^2}j_{2\nu}(l_2, l_2') \times \frac{iN^{\nu\nu'}(k_2)}{k_2^2 - m_2^2}\mathcal{M}^{\mathcal{W}}_{\mu'\nu'}. \tag{33}$$

We decompose the two propagator matrices in (33) according to (31), (32). Then the matrix element (33) takes the same form as the corresponding matrix element (7). Therefore the computation of the cross section of $f_1f_2 \to f_1'f_2'\mathcal{W}$ in the IEVBA in the axial gauge proceeds as the derivation in the unitary gauge in Sec. II. What is different now is the modeling of the relation between the off-shell and on-shell cross section for $V_1V_2 \to \mathcal{W}$. Because the longitudinal polarization vectors $\varepsilon_i^\mu(0)$ do not contain kinematic singularities at $k_i^2 = 0$ we use, instead of (20), the approximation

$$\tilde{\sigma}^{\mathrm{axial}}_{\mathrm{pol}}(\hat{s}, k_1^2, k_2^2) \approx \hat{\sigma}_{\mathrm{pol}}(\hat{s}, m_1^2, m_2^2), \tag{34}$$

where $\hat{\sigma}_{\mathrm{pol}}$ is the on-shell $V_1V_2 \to \mathcal{W}$ cross section, which is gauge-independent. That is, we put all the factors $f_{\mathrm{pol}} = 1$. In our view, there is no physical argument for using in the axial gauge factors $f_{\mathrm{pol}} \neq 1$ in the extrapolation of the off-shell hard scattering cross section to the on-shell cross section, as done in the unitary gauge.

The IEVBA approximation to the cross section of $f_1f_2 \to f_1'f_2'\mathcal{W}$ is then given, in analogy to (23), by

$$\sigma^{\mathrm{IEVBAaxial}}_{f_1f_2\to f_1'f_2'\mathcal{W}} = \sum_{\mathrm{pol}}\int_{x_{\min}}^1 dx\mathbf{L}^{\mathrm{axial}}_{\mathrm{pol}}(x)\hat{\sigma}_{\mathrm{pol}}(\hat{s} = xs, m_1^2, m_2^2), \tag{35}$$

where $\mathbf{L}^{\mathrm{axial}}_{\mathrm{pol}}(x)$ is obtained from (24) using $f_{\mathrm{pol}} = 1$ and $\mathcal{J}^{\mathrm{axial}}_{\mathrm{pol}}$. In turn the differential luminosities $\mathcal{J}^{\mathrm{axial}}_{\mathrm{pol}}$ are determined by the integral (25) of $\mathcal{L}^{\mathrm{axial}}_{\mathrm{pol}}$. These quantities are defined as in (17) with the form factors $\mathcal{C}_i, \mathcal{S}_i$ defined in (16) to be computed in the axial gauge. One can choose the two sets of transverse polarization vectors $\varepsilon_i^\mu(\pm1)$ to be identical to those in the unitary gauge if n^μ is appropriately chosen. Then only those (differential) luminosities change with respect to the corresponding ones in Sec. II where the label "pol" contains at least one index L. We compute the axial-gauge form factors $\mathcal{C}_1(0)$ and $\mathcal{C}_2(0)$ in the Breit frames B_1 and B_2, respectively, which were defined below (21). For definiteness we choose in the following n^μ to be lightlike, and we use $n^\mu = (1, 0, 0, -1)$ in the V_1V_2 center-of-mass frame. According to [21] a lightlike n^μ yields the best approximation to the cross-section ratio $\sigma^{\mathrm{EVBA}}/\sigma^{\mathrm{full}}$ for $f_1f_2 \to f_1'f_2'W^+W^-$. For this choice of n^μ the polarization

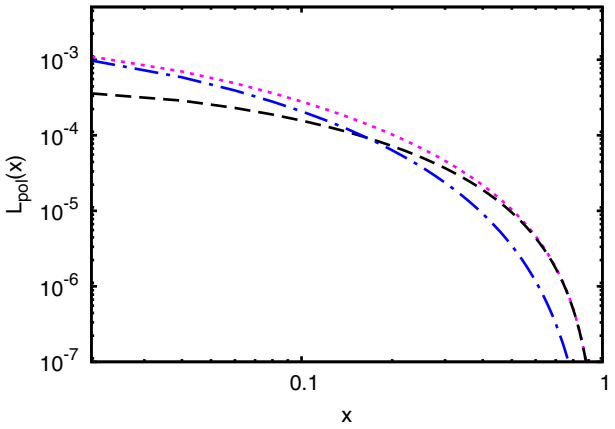

FIG. 4. The luminosities $\mathbf{L}_{\mathrm{LL}}^{\mathrm{axial}}(x)$ (dot-dashed blue), $\mathbf{L}_{\mathrm{LT}}^{\mathrm{axial}}(x)$ (dotted magenta), and $\mathbf{L}_{\mathrm{L\overline{T}}}^{\mathrm{axial}}(x)$ (dashed black) for a W^-W^+ pair in e^-e^+ collisions at $\sqrt{s} = 2$ TeV.

vectors $\epsilon_i^\mu(0)$ are given in Appendix B in the V_1V_2 center-of-mass frame and in the frames B_i. Moreover, in this appendix we list also those $\mathcal{J}_{\mathrm{pol}}^{\mathrm{axial}}$ which differ from their counterparts in the unitary gauge. In the following the term "axial gauge" refers to this choice of n^μ.

Let us now consider, in analogy to Sec. II, the luminosities $\mathbf{L}_{\mathrm{pol}}^{\mathrm{axial}}(x)$ of finding a W^-W^+ pair in unpolarized e^-e^+ collisions at $\sqrt{s} = 2$ TeV. As mentioned above, $\mathbf{L}_{\mathrm{TT}}^{\mathrm{axial}}$, $\mathbf{L}_{\mathrm{\overline{T}\overline{T}}}^{\mathrm{axial}}$, and $\mathbf{L}_{\mathrm{T\overline{T}}}^{\mathrm{axial}} = -\mathbf{L}_{\mathrm{\overline{T}T}}^{\mathrm{axial}}$ are identical to those in the unitary gauge shown in Figs. 2 and 3. The other luminosities are plotted in Fig. 4 where the same parameter values as in Sec. II were used. The relations (28) hold also in the axial gauge. Moreover, $\mathbf{L}_{\mathrm{TL}}^{\mathrm{axial}}(x) = \mathbf{L}_{\mathrm{LT}}^{\mathrm{axial}}(x)$.

Comparing the luminosities displayed in Fig. 4 with the corresponding ones in Figs. 2 and 3 we get the following. The luminosity $\mathbf{L}_{\mathrm{LL}}^{\mathrm{axial}}(x)$ is larger than $\mathbf{L}_{\mathrm{LL}}(x)$ by a factor ~ 3 for $x \sim 0.01$–0.2. The ratio of these two luminosities increases to ~ 7 for $x \gtrsim 0.6$. The luminosities $\mathbf{L}_{\mathrm{LT}}^{\mathrm{axial}}(x)$, $\mathbf{L}_{\mathrm{L\overline{T}}}^{\mathrm{axial}}(x)$ are larger than the corresponding ones in the unitary gauge by a factor of ~ 2–3. This is mainly due to the fact that in the axial gauge the factors (21) were not taken into account which suppress the unitary-gauge luminosities in the region $|k_i^2| > m_i^2$.

IV. APPLICATIONS AND COMPARISON WITH FULL COMPUTATIONS

In this section we analyze the quality of the improved effective vector boson approximation—that is, the quality of the formulas (23) and (35)—for the production cross section of W^-W^+ bosons and top-quark top antiquark $(t\bar{t})$ pairs at high energies. To be specific we consider the processes $e^-e^+ \to W^-W^+\nu_e\overline{\nu}_e$ and $e^-e^+ \to t\bar{t} + \nu_e\overline{\nu}_e$ in the Standard Model and compute the tree-level cross sections both in the IEVBA using the weak-boson pair luminosities determined above in the unitary and axial gauge and fully, that is, taking all SM contributions into account, with the computer code MadGraph [26]. We determine the relative deviation of the IEVBA from the respective full cross section in dependence of several phase-space cuts. In both examples, nondiagonal interference contributions are not taken into account. As mentioned above, in our view the IEVBA loses its simplicity and appeal with these nondiagonal contributions.

Besides the weak gauge-boson masses stated above, we use $m_H = 125$ GeV, $m_t = 173$ GeV, and $m_b = 4.7$ GeV for the Higgs-boson, top-quark, and b-quark mass, respectively.

A. $e^-e^+ \to W^-W^+\nu_e\overline{\nu}_e$

We consider the reaction

$$e^-e^+ \to W^-W^+\nu_e\overline{\nu}_e \tag{36}$$

for unpolarized e^-e^+ collisions and center-of-mass energies $\sqrt{s}$ in the TeV range. At tree-level in the SM there are 56 diagrams that contribute to (36), while in the effective vector boson approximation 7 diagrams contribute to the hard scattering reactions $W^-W^+ \to W^-W^+$. Within the IEVBA the cross section for (36), summed over the helicities of the final-state W^-W^+, is given in the unitary gauge by

$$\sigma_{W^-W^+}^{\mathrm{IEVBA}}(s) = \sum_{\mathrm{pol}} \int_{x_{\min}}^1 \mathrm{d}x \mathbf{L}_{\mathrm{pol}}(x) \hat{\sigma}_{\mathrm{pol}}^{W^-W^+}(\hat{s} = xs, m_W^2, m_W^2), \tag{37}$$

where the sum extends over $\mathrm{pol} = \mathrm{TT}, \overline{\mathrm{TT}}, \mathrm{TL}, \mathrm{LT}, \mathrm{LL}$. An analogous formula holds in the axial gauge. Because at lowest order in the SM the scattering amplitude of $W^-W^+ \to W^-W^+$ is not affected by parity violation, the terms $\tilde{\sigma}_{\mathrm{pol}}^{W^-W^+} = 0$ for $\mathrm{pol} = \overline{\mathrm{T}}\overline{\mathrm{T}}, \mathrm{T}\overline{\mathrm{T}}, \mathrm{L}\overline{\mathrm{T}}$, and $\overline{\mathrm{T}}\mathrm{L}$. We define the relative deviation of (37) from the full tree-level cross section $\sigma_{W^-W^+}^{\mathrm{full}}$ computed with MadGraph [26] and the corresponding deviation in the axial gauge by

$$\delta_{WW} = \frac{\sigma_{W^-W^+}^{\mathrm{IEVBA}} - \sigma_{W^-W^+}^{\mathrm{full}}}{\sigma_{W^-W^+}^{\mathrm{full}}},$$
$$\delta_{WW}^{\mathrm{axial}} = \frac{\sigma_{W^-W^+}^{\mathrm{IEVBA,axial}} - \sigma_{W^-W^+}^{\mathrm{full}}}{\sigma_{W^-W^+}^{\mathrm{full}}}. \tag{38}$$

In the following we choose $\sqrt{s} = 2$ TeV. The (improved) effective vector boson approximation is known to significantly overestimate the cross section for the reaction (36) unless appropriate cuts on kinematic variables of $W^\mp$ are made. We require a minimum value M^* of the invariant mass $M_{WW} \equiv \hat{s}$ of the final-state W^-W^+ pair. First we analyze the quality of the IEVBA for W^-W^+ production in the central region. We compute, for fixed M^* the relative

TABLE I. Relative deviations $\delta_{WW}(M_{WW} \geq M^*)$ and $\delta_{WW}^{\text{axial}}(M_{WW} \geq M^*)$ defined in (38) of the IEVBA cross section from the full result for $e^-e^+ \to W^-W^+\nu\bar{\nu}$ at $\sqrt{s} = 2$ TeV for several upper cuts y_W^* on the moduli of the $W^\mp$-boson rapidities in the laboratory frame. The additional cut $p_{T,W} > 20$ GeV on the transverse momentum of the W bosons was applied.

y_W^*	2.5	2	1.8	1.7	1.6	1.5
$\delta_{WW}(M_{WW} \geq 400\ \text{GeV})$	3.05	0.95	0.33	0.08	−0.12	−0.26
$\delta_{WW}(M_{WW} \geq 500\ \text{GeV})$	3.22	0.71	0.11	−0.06	−0.17	−0.27
$\delta_{WW}(M_{WW} \geq 600\ \text{GeV})$	3.20	0.45	0.05	−0.07	−0.18	−0.26
$\delta_{WW}^{\text{axial}}(M_{WW} \geq 400\ \text{GeV})$	5.15	1.84	0.86	0.48	0.17	−0.03
$\delta_{WW}^{\text{axial}}(M_{WW} \geq 500\ \text{GeV})$	5.35	1.38	0.45	0.21	0.05	−0.06
$\delta_{WW}^{\text{axial}}(M_{WW} \geq 600\ \text{GeV})$	5.22	0.90	0.34	0.17	0.04	−0.06

deviations δ_{WW} and $\delta_{WW}^{\text{axial}}$ for a sequence of upper cuts y_W^* on the moduli of the W^-- and W^+-boson rapidities in the laboratory frame; i.e., we restrict $|y_W| \leq y_W^*$. The implementation of this cut is described in Appendix A. The computation of the elastic $W^-W^+ \to W^-W^+$ cross section requires a cut in order to avoid the t-channel photon-propagator pole. Here we use a cut on the transverse momentum of the W bosons, $p_{T,W} > 20$ GeV. The same set of cuts is also applied to the calculation of $\sigma_{W^-W^+}^{\text{full}}$.

The resulting values of δ_{WW} given in Table I show that the size of the relative deviation depends quite sensitively on the rapidity cut. For loose cuts y_W^* the cross section computed in the IEVBA approximation is larger than the exact value, while it is the other way around for very tight upper cuts on $|y_W|$. In the latter case the cross section is, however, reduced significantly. Table I shows that the IEVBA approximation agrees within ∼10% with the full calculation if $|y_W|$ is restricted to values less than ∼1.7. The upper cut on $|y_W|$ can be loosened if the cut M^* is increased. However, as the numbers in Table I show, $|\delta_{WW}|$ increases again below $|y_W| = 1.7$. For $|y_W| < 1.5$ the ratio $\delta_{WW} \simeq -.30$. For these tight cuts the event numbers rapidly decrease.

As mentioned in Sec. II the luminosity $\mathbf{L}_{\overline{\text{T}}\overline{\text{T}}}(x)$ was given in [15] with the wrong sign. With the correct luminosities and with the set of cuts used in Table I, the approximation $\sigma_{W^-W^+}^{\text{IEVBA}}$ improves by 1% for $|y_W| < 2.5$. The improvement increases to 9% for $|y_W| \lesssim 1.7$.

The corresponding ratios $\delta_{WW}^{\text{axial}}$, which are given also in Table I, show that for loose upper cuts on $|y_W|$ the IEVBA approximation in the axial gauge is worse than in the unitary gauge. This stems from the fact that in the axial gauge we have put all factors $f_{\text{pol}} = 1$ (cf. Sec. III) which generates in this kinematic regime larger contributions to $\sigma_{W^-W^+}^{\text{IEVBA,axial}}$ with labels pol = TL, LT, LL. Only for $|y_W| \lesssim 1.6$ the axial-gauge IEVBA provides a relatively good approximation to the full cross section.

TABLE II. Same as Table I, but $\delta_{WW}(M_{WW} \geq M^*)$ for several minimum cuts $p_{T,W}^*$ on the transverse momentum of the $W^\mp$ boson and the cut $|y_W| \leq 2$.

$p_{T,W}^*$ [GeV]	100	150	200	250	300
$\delta_{WW}(M_{WW} \geq 400\ \text{GeV})$	0.359	0.347	0.271	0.089	−0.105
$\delta_{WW}(M_{WW} \geq 500\ \text{GeV})$	0.440	0.395	0.312	0.130	−0.087
$\delta_{WW}(M_{WW} \geq 600\ \text{GeV})$	0.488	0.439	0.315	0.128	−0.068
$\delta_{WW}^{\text{axial}}(M_{WW} \geq 400\ \text{GeV})$	0.746	0.684	0.552	0.314	0.069
$\delta_{WW}^{\text{axial}}(M_{WW} \geq 500\ \text{GeV})$	0.843	0.740	0.603	0.363	0.089
$\delta_{WW}^{\text{axial}}(M_{WW} \geq 600\ \text{GeV})$	0.890	0.786	0.607	0.362	0.113

Next we analyze δ_{WW} and $\delta_{WW}^{\text{axial}}$ in dependence of a minimum cut on the transverse momentum of the $W^\mp$ boson. In addition a cut $|y_W| \leq 2$ on the $W^\mp$ rapidity is applied. The results given in Table II exhibit that the unitary-gauge IEVBA approximates the exact cross section to ∼10% only if a cut $p_{T,W} \geq 250$ GeV is imposed. The additional cut on the $W^\mp$ rapidity improves the quality of the IEVBA only for $p_{T,W} \lesssim 200$ GeV. In the kinematic regime considered here the IEVBA in the axial gauge is in general worse than in the unitary gauge, for reasons mentioned above. Only for very hard cuts on $p_{T,W}$ the axial-gauge IEVBA works reasonably well.

B. $e^-e^+ \to t\bar{t}\nu_e\bar{\nu}_e$

As a further reaction of interest, we investigate the cross section of

$$e^-e^+ \to t\bar{t}\nu_e\bar{\nu}_e \tag{39}$$

for unpolarized e^-e^+ collisions. In the standard model twenty-one tree-level Feynman diagrams contribute to (39) while in the IEVBA the hard-scattering subprocess $W^-W^+ \to t\bar{t}$ receives four diagram contributions. The cross section of (39) in the IEVBA in the unitary gauge is

$$\sigma_{t\bar{t}}^{\text{IEVBA}}(s) = \sum_{\text{pol}} \int_{x_{\min}}^1 \mathrm{d}x \mathbf{L}_{\text{pol}}(x) \hat{\sigma}_{\text{pol}}^{t\bar{t}}(\hat{s} = xs, m_W^2, m_W^2). \tag{40}$$

Here the sum extends over all nine polarization labels introduced in (17). That is, also the four luminosities and $\tilde{\sigma}_{\text{pol}}^{t\bar{t}}$ that involve a parity-odd combination of vector and axial vector couplings contribute. This is because of the relations (28) and

$$\hat{\sigma}_{\overline{\text{T}}\text{T}}^{t\bar{t}}(x) = -\hat{\sigma}_{\text{T}\overline{\text{T}}}^{t\bar{t}}(x), \qquad \hat{\sigma}_{\overline{\text{T}}\text{L}}^{t\bar{t}}(x) = -\hat{\sigma}_{\text{L}\overline{\text{T}}}^{t\bar{t}}(x), \tag{41}$$

which follow from CP invariance. A formula analogous to (40) holds for the IEVBA in the axial gauge.

In analogy to (38) we define the relative deviation $\delta_{t\bar{t}}$ of (40) and the analogous ratio $\delta_{t\bar{t}}^{\text{axial}}$ from the full tree-level

TABLE III. Relative deviations $\delta_{t\bar{t}}(M_{t\bar{t}} \geq M^*)$ and $\delta_{t\bar{t}}^{\text{axial}}$ defined in analogy to (38) of the IEVBA cross section from the full result for $e^-e^+ \to t\bar{t}\nu\bar{\nu}$ at $\sqrt{s} = 2$ TeV for several upper cuts y_t^* on the moduli of the t and $\bar{t}$ rapidities in the laboratory frame.

y_t^*	5	4	3	2	1.5	1
$\delta_{t\bar{t}}(M_{t\bar{t}} \geq 400\ \text{GeV})$	0.090	0.090	0.090	0.076	0.011	−0.081
$\delta_{t\bar{t}}(M_{t\bar{t}} \geq 500\ \text{GeV})$	0.064	0.064	0.064	0.045	−0.048	−0.180
$\delta_{t\bar{t}}(M_{t\bar{t}} \geq 600\ \text{GeV})$	0.006	0.005	0.004	−0.024	−0.154	−0.296
$\delta_{t\bar{t}}^{\text{axial}}(M_{t\bar{t}} \geq 400\ \text{GeV})$	3.18	3.18	3.17	3.11	2.78	2.36
$\delta_{t\bar{t}}^{\text{axial}}(M_{t\bar{t}} \geq 500\ \text{GeV})$	3.47	3.47	3.47	3.38	2.91	2.31
$\delta_{t\bar{t}}^{\text{axial}}(M_{t\bar{t}} \geq 600\ \text{GeV})$	3.55	3.55	3.55	3.42	2.74	2.04

cross section $\sigma_{t\bar{t}}^{\text{full}}$ computed with MadGraph. We choose $\sqrt{s} = 2$ TeV and use the same set of minimum values M^* as in Sec. IV A, now for the invariant mass $M_{t\bar{t}} \equiv \hat{s}$ of the $t\bar{t}$ pair.

First we analyze the quality of the IEVBA in the unitary gauge. In Table III the relative deviation $\delta_{t\bar{t}}$ is given for a sequence of upper cuts y_t^* on the moduli of the t and $\bar{t}$ rapidities in the laboratory frame. For rather loose cuts a precision of about 10% or better can be obtained. However, similar to the example analyzed in subsection IV A, the y_t^* region where $\delta_{t\bar{t}}$ becomes minimal is correlated with the value of the cut on the $t\bar{t}$ invariant mass. We remark that the improvements discussed in Sec. II [i.e., correct sign of $\mathbf{L}_{\overline{\text{TT}}}$ and including the contributions to (40) with parity-odd combinations of vector and axial vector couplings] improves the quality of the IEVBA by about 20% (30%) for loose cuts ($y_t^* \lesssim 2$).

In addition, we analyze $\delta_{t\bar{t}}$ in dependence of a minimum cut $p_{T,t}^*$ on the transverse momentum of the t and $\bar{t}$ quarks. The numbers given in Table IV show that for $t\bar{t}$ events with $M_{t\bar{t}} \geq 500$ GeV and a moderate transverse momentum cut $p_{T,t} \geq 50$ GeV a precision of about 10% or better, depending on the value of M^*, can be obtained.

The numbers for $\delta_{t\bar{t}}^{\text{axial}}$ given in Tables III and IV show that in the kinematic regimes considered the IEVBA approximation (40) in the axial gauge overestimates the full result by a factor of about 3 to 4. The reason is that the on-shell hard scattering cross sections $\hat{\sigma}_{\text{pol}}^{t\bar{t}}$ are dominated by those where W^- and/or W^+ is longitudinally polarized and the associated axial-gauge luminosities $\mathbf{L}_{\text{pol}}$ are significantly larger than those in the unitary gauge. If one chooses tighter cuts than those used in Tables III and IV the deviations $\delta_{t\bar{t}}^{\text{axial}}$ diminish, but at the cost of rapidly decreasing event numbers.

TABLE IV. Same as Table III, but $\delta_{t\bar{t}}(M_{t\bar{t}} \geq M^*)$ for several minimum cuts $p_{T,t}^*$ on the t and $\bar{t}$ transverse momentum.

$p_{T,t}^*$ [GeV]	0	50	100	150	200
$\delta_{t\bar{t}}(M_{t\bar{t}} \geq 400\ \text{GeV})$	0.090	0.108	0.119	0.027	−0.099
$\delta_{t\bar{t}}(M_{t\bar{t}} \geq 500\ \text{GeV})$	0.064	0.043	0.005	0.010	−0.068
$\delta_{t\bar{t}}(M_{t\bar{t}} \geq 600\ \text{GeV})$	0.005	−0.043	−0.110	−0.144	−0.163
$\delta_{t\bar{t}}^{\text{axial}}(M_{t\bar{t}} \geq 400\ \text{GeV})$	3.18	3.27	3.37	3.20	2.83
$\delta_{t\bar{t}}^{\text{axial}}(M_{t\bar{t}} \geq 500\ \text{GeV})$	3.47	3.38	3.21	3.21	2.97
$\delta_{t\bar{t}}^{\text{axial}}(M_{t\bar{t}} \geq 600\ \text{GeV})$	3.55	3.33	2.99	2.80	2.67

Our results for the reactions (36) and (39) show that the unitary-gauge IEVBA provides a relatively good approximation to the full cross section if hard cuts on $|y_W|$ and $p_{T,W}$ are applied, while the axial-gauge IEVBA is worse in general. Given a specific choice of cuts it is not possible to make a quantitative *a priori* estimate of the quality of the IEVBA. What could then be the use of the IEVBA—in particular, in view of the fact that computer codes such as those of [25,26] allow us to compute tree-level cross sections exactly? One potential application, which keeps the computational effort at bay, is to calculate the tree-level cross section fully by taking into account all contributing Feynman diagrams but to implement the radiative corrections to the respective hard scattering process $V_1V_2 \to \mathcal{W}$ using the IEVBA. In Ref. [22] this strategy was pursued with the unitary-gauge IEVBA for the reaction (36) and it was argued that this leads to quantitatively satisfactory results.

V. SUMMARY AND CONCLUSIONS

We revisited the improved effective vector boson approximation [15] in the unitary gauge that was designed to catch the essence of weak gauge boson scattering $V_1V_2 \to \mathcal{W}$ in high-energy pp and e^-e^+ collisions with an improved precision compared to the EVBA in the leading logarithmic approximation. We computed the correlated two-vector-boson luminosities $\mathbf{L}_{\text{pol}}(x)$ for V_1, V_2 being radiated off a massless quark or lepton f_1 and f_2, respectively, for the nine combinations of the transverse and longitudinal polarizations of V_1 and V_2. We clarified a sign issue that appears in some of the $\mathbf{L}_{\text{pol}}(x)$. Our results for the parity-even luminosities $\mathbf{L}_{\text{pol}}(x)$ agree with those of [15], up to a sign in the case of $\mathbf{L}_{\overline{\text{TT}}}$. Our results for the four luminosities that involve a parity-odd combination of vector and axial vector couplings were, to our knowledge, so far not available in the literature. They are required if the hard scattering amplitude of $V_1V_2 \to \mathcal{W}$ is affected also by

parity-violating interactions. For instance, this is the case for $V_1V_2 \to ff'$ where f, f' are heavy quarks or leptons. We computed also the correlated two-vector-boson luminosities $\mathbf{L}^{\text{axial}}_{\text{pol}}(x)$ in the axial gauge, using a specific vector n^ν.

Furthermore, we studied the reactions $e^-e^+ \to W^-W^+\nu_e\overline{\nu}_e$ and $e^-e^+ \to t\bar{t}\nu_e\overline{\nu}_e$ within the standard model for large e^-e^+ center-of-mass energies by computing the respective tree-level cross section using the IEVBA in the unitary and axial gauge and comparing these approximations with the full SM cross section computed with MadGraph [26]. Here, our aim was to probe the quality of the formulas (23) and (35). We found that the IEVBA in the unitary gauge provides a relatively good approximation to the full cross section if hard cuts on the rapidities and transverse momenta of the W^-, W^+, respectively t, $\bar{t}$ in the final state are applied. In the case of $t\bar{t}$ the inclusion of the luminosities with parity-odd combinations of vector and axial vector couplings improves the quality of the IEVBA by 20–30% depending on the chosen cuts. Using the axial-gauge luminosities the IEVBA becomes worse in general, for reasons discussed above.

The applicability of the (improved) effective vector boson approximation is certainly limited because, for a given high-energy reaction and a choice of cuts, it seems not possible to quantify *a priori* the precision of the approximation. At best one may use the IEVBA, which is gauge dependent, for a semiquantitative estimate of the effect of the hard scattering process $V_1V_2 \to \mathcal{W}$. For instance, one may use it to estimate the effect of radiative corrections to this subprocess, as mentioned at the end of Sec. IV. The IEVBA may also be useful if new physics effects are considered and if the new physics effects on $V_1V_2 \to \mathcal{W}$ are dominated by one or a few helicity combinations of the weak gauge bosons.

ACKNOWLEDGMENTS

We wish to thank Hubert Spiesberger for discussions. Long Chen is supported by a scholarship from the China Scholarship Council (CSC).

APPENDIX A: FOUR-FOLD DIFFERENTIAL LUMINOSITIES IN THE UNITARY GAUGE

Here we give explicit expressions for the nine differential luminosities $\mathcal{J}_{\text{pol}}$ in the unitary gauge defined in (25). They are calculated as follows. One starts with the center-of-mass frame of the off-shell vector bosons V_1 and V_2 whose four-momenta are given by

$$k_1^\mu = (k_{01}, 0, 0, k), \qquad k_2^\mu = (k_{02}, 0, 0, -k). \tag{A1}$$

In this frame the polarization vectors of V_1 and V_2 in the unitary gauge of helicity λ_1 and λ_2, respectively, are given in the Jacob-Wick phase conventions:

$$\varepsilon_1^\mu(\pm) = \frac{1}{\sqrt{2}}(0, \mp 1, -i, 0),$$
$$\varepsilon_1^\mu(0) = \frac{1}{\sqrt{-k_1^2}}(k, 0, 0, k_{01}), \tag{A2}$$

$$\varepsilon_2^\mu(\pm) = \frac{1}{\sqrt{2}}(0, \pm 1, -i, 0),$$
$$\varepsilon_1^\mu(0) = \frac{1}{\sqrt{-k_2^2}}(-k, 0, 0, k_{02}). \tag{A3}$$

As already mentioned below Eq. (21) the four-momentum and polarization vectors of V_1 (V_2) and the four-momenta of f_1, f_1' (f_2, f_2') are Lorentz-transformed into the Breit frame B_1 (B_2) where the form factors $\mathcal{C}_1$, $\mathcal{S}_1$ $(\mathcal{C}_2, \mathcal{S}_2)$ defined in (16) are conveniently computed. They determine the $\mathcal{L}_{\text{pol}}$ defined in (17). Performing the integration over the azimuthal angles in (25) we obtain the differential luminosities $\mathcal{J}_{\text{pol}}$. For the sake of brevity we omit details of the computation; they are given in [15].

For fixed squared center-of-mass energy $\sqrt{s}$ of the initial fermions f_1, f_2 the $\mathcal{J}_{\text{pol}}$ are functions of k_1^2, k_2^2 and the variables x and u defined in (10) and (22), respectively. We obtain for the reactions (1):

$$\mathcal{J}_{\text{TT}} = c_{\text{TT}}\left(1 + \frac{4(u-\nu)^2}{\kappa^2}\right)\left(\frac{1}{2} + \frac{s(s-u)}{u^2} + \frac{k_1^2k_2^2}{\kappa^2u^4}(k_1^2k_2^2 + u^2 - 2u\nu)(u^2 - 6us + 6s^2)\right), \tag{A4}$$

$$\mathcal{J}_{\text{LT}} = c_{\text{LT}}\left(1 + \frac{4(u-\nu)^2}{\kappa^2}\right)\left(\frac{s(s-u)}{u^2} + \frac{k_1^2k_2^2}{\kappa^2u^4}(k_1^2k_2^2 + u^2 - 2u\nu)(u^2 - 6us + 6s^2)\right), \tag{A5}$$

$$\mathcal{J}_{\text{TL}} = c_{\text{TL}}\left(-1 + \frac{4(u-\nu)^2}{\kappa^2}\right)\left(\frac{1}{2} + \frac{s(s-u)}{u^2} + \frac{k_1^2k_2^2}{\kappa^2u^4}(k_1^2k_2^2 + u^2 - 2u\nu)(u^2 - 6us + 6s^2)\right), \tag{A6}$$

$$\mathcal{J}_{\overline{\text{T}}\overline{\text{T}}} = (-1)^{r_1+r_2}\frac{4c_{\overline{\text{T}}\overline{\text{T}}}}{\kappa^2u^2}(u-\nu)(k_1^2k_2^2 - u\nu)(u-2s), \tag{A7}$$

$$\mathcal{J}_{\overline{\text{T}}\overline{\text{T}}} = (-1)^{r_1}c_{\overline{\text{T}}\overline{\text{T}}}\left(1 + \frac{4(u-\nu)^2}{\kappa^2}\right)\frac{k_1^2k_2^2 - u\nu}{\kappa u^2}(u-2s), \tag{A8}$$

$$\mathcal{J}_{\text{T}\overline{\text{T}}} = (-1)^{r_2}4c_{\text{T}\overline{\text{T}}}\frac{(u-\nu)}{\kappa}\left(\frac{1}{2} + \frac{s(s-u)}{u^2} + \frac{k_1^2k_2^2}{\kappa^2u^4}(k_1^2k_2^2 + u^2 - 2u\nu)(u^2 - 6us + 6s^2)\right), \tag{A9}$$

$$\mathcal{J}_{\overline{\mathrm{TL}}} = (-1)^{r_1} c_{\overline{\mathrm{TL}}} \left(-1 + \frac{4(u-\nu)^2}{\kappa^2}\right) \frac{k_1^2 k_2^2 - u\nu}{\kappa u^2} (u - 2s), \tag{A10}$$

$$\mathcal{J}_{\mathrm{L}\overline{\mathrm{T}}} = (-1)^{r_2} 4 c_{\mathrm{L}\overline{\mathrm{T}}} \frac{(u-\nu)}{\kappa} \left(\frac{s(s-u)}{u^2} + \frac{k_1^2 k_2^2}{\kappa^2 u^4} (k_1^2 k_2^2 + u^2 - 2u\nu)(u^2 - 6us + 6s^2)\right), \tag{A11}$$

$$\mathcal{J}_{\mathrm{LL}} = c_{\mathrm{LL}} \left(-1 + \frac{4(u-\nu)^2}{\kappa^2}\right) \left(\frac{s(s-u)}{u^2} + \frac{k_1^2 k_2^2}{\kappa^2 u^4} (k_1^2 k_2^2 + u^2 - 2u\nu)(u^2 - 6us + 6s^2)\right), \tag{A12}$$

where the variables ν and κ are given in (27) and the powers r_1, r_2, which are either zero or one, are defined below Eq. (16). In (A4)–(A12) we have used the abbreviations

$$\begin{aligned} &c_{\mathrm{TT}} = c_{\mathrm{LT}} = c_{\mathrm{TL}} = c_{\mathrm{LL}} = (v_1^2 + a_1^2)(v_2^2 + a_2^2), \\ &c_{\mathrm{T}\overline{\mathrm{T}}} = c_{\mathrm{L}\overline{\mathrm{T}}} = 2(v_1^2 + a_1^2) v_2 a_2, \\ &c_{\overline{\mathrm{T}}\mathrm{T}} = c_{\overline{\mathrm{TL}}} = 2(v_2^2 + a_2^2) v_1 a_1, \\ &c_{\overline{\mathrm{TT}}} = 4 v_1 a_1 v_2 a_2, \end{aligned} \tag{A13}$$

where v_i, a_i are the vector and axial vector coupling of the intermediate gauge boson V_i which are defined below Eq. (16).

If no phase-space cuts are applied and if one integrates over the variable u and defines $\tilde{\mathcal{J}}_{\mathrm{pol}} = \int_{\hat{x}s}^{s} (du/u) \mathcal{J}_{\mathrm{pol}}$, then the following relations hold in the physical region defined by the integration regions over the remaining phase-space variables in (23), (24):

$$\begin{aligned} &\tilde{\mathcal{J}}_{\mathrm{TL}} = \tilde{\mathcal{J}}_{\mathrm{LT}}, \qquad \tilde{\mathcal{J}}_{\mathrm{T}\overline{\mathrm{T}}} = (-1)^{r_2 - r_1} \frac{c_{\mathrm{T}\overline{\mathrm{T}}}}{c_{\overline{\mathrm{TT}}}} \tilde{\mathcal{J}}_{\overline{\mathrm{TT}}}, \\ &\tilde{\mathcal{J}}_{\mathrm{L}\overline{\mathrm{T}}} = (-1)^{r_2 - r_1} \frac{c_{\mathrm{L}\overline{\mathrm{T}}}}{c_{\overline{\mathrm{TL}}}} \tilde{\mathcal{J}}_{\overline{\mathrm{TL}}}. \end{aligned} \tag{A14}$$

Finally, we describe how cuts can be applied on the rapidities of the particles in the final state $\mathcal{W}$ of the reactions (1). We introduce the variables

$$z \equiv \frac{u + k_1^2}{s} = \frac{2k_1 \cdot l_2 + k_1^2}{2l_1 \cdot l_2}, \qquad K^2 \equiv \frac{u + k_1^2}{u} k_2^2. \tag{A15}$$

In terms of these variables the three-dimensional integration measure in (24) is

$$\int_{-s+\hat{s}}^{0} \mathrm{d}k_1^2 \int_{-s+\hat{s}'}^{0} \mathrm{d}k_2^2 \int_{\hat{x}s}^{s} \frac{\mathrm{d}u}{u} = \int_x^1 \frac{\mathrm{d}z}{z} \int_{-s(1-z)}^{0} \mathrm{d}k_1^2 \int_{-s(z-x)}^{0} \mathrm{d}K^2. \tag{A16}$$

In the context of the effective vector boson approximation the dominant kinematic configuration corresponds to the intermediate vector boson V_1 and V_2 moving collinear to the $f_1 f_2$ beam axis. Then the variable z defined in (A15) is approximately equal to the longitudinal momentum fraction of V_1 with respect to f_1. Analogously we denote by z' the longitudinal momentum fraction of V_2 with respect to f_2. The longitudinal velocity of the intermediate vector-boson pair $V_1 V_2$ in the $f_1 f_2$ center-of-mass frame is $\beta_{V_1 V_2} = (z - z')/(z + z')$, and the rapidity of the pair is

$$y_{V_1 V_2} = \frac{1}{2} \ln\left(\frac{1 + \beta_{V_1 V_2}}{1 - \beta_{V_1 V_2}}\right) = \frac{1}{2} \ln\left(\frac{z^2}{x}\right). \tag{A17}$$

We consider now a particle F in the final state $\mathcal{W}$ of the reaction (1). [In the examples analyzed in Sec. IV F corresponds to a W boson or an (anti)top quark.] The rapidity of F in the $f_1 f_2$ center-of-mass frame is given by

$$y_F = y_{V_1 V_2} + y'_F, \tag{A18}$$

where $y'_F = (1/2) \ln[(E'_F + p'_{3F})/(E'_F - p'_{3F})]$ is the rapidity of F in the $V_1 V_2$ center-of-mass frame. Cuts on y_F can be implemented using (A16) and (A18).

APPENDIX B: FOUR-FOLD DIFFERENTIAL LUMINOSITIES IN THE AXIAL GAUGE

Here we list explicit expressions for those differential luminosities that differ from their counterparts in the unitary gauge. For definiteness, we choose n^μ to be lightlike. In the $V_1 V_2$ center-of-mass frame we use $n^\mu = (0, 0, 0, -1)$. In this frame the four-momenta of V_1 and V_2 are given by (A1) and their transverse polarization vectors can be chosen to be those listed in (A2), (A3). Using (32) and $n^2 = 0$ the longitudinal polarization vectors in this frame are

$$\varepsilon_i^\mu(0) = \sqrt{\frac{-k_i^2}{(k_i \cdot n)^2}} n^\mu, \quad i = 1, 2. \tag{B1}$$

As was done in Appendix A the four-momentum and polarization vectors of V_1 (V_2) and the four-momenta of f_1, f_1' (f_2, f_2') are Lorentz-transformed into the Breit frame B_1 (B_2). We obtain for the longitudinal polarization vectors of V_1 and V_2:

$$
\begin{aligned}
(\varepsilon_1^{B_1})^\mu(0) &= h_1(e_0, e_1, 0, e_3),\\
h_1 &= \frac{2\sqrt{-k_1^2}}{\kappa},\\
e_0 &= \frac{1}{\sqrt{-k_1^2}}\left(\nu - \frac{k_1^2 k_2^2}{u}\right),\\
e_1 &= \frac{\sqrt{-k_2^2}}{u}\sqrt{k_1^2 k_2^2 + u(u-2\nu)},\\
e_3 &= -\frac{\kappa}{2\sqrt{-k_1^2}},\\
(\varepsilon_2^{B_2})^\mu(0) &= (1,0,0,1).
\end{aligned}
\tag{B2}
$$

The variables u, ν, and κ are defined in (22) and (27). The transverse polarization vectors of V_1 (V_2) and the four-momenta of V_1, f_1, f_1' (V_2, f_2, f_2') in B_1 (B_2) are given in Appendix A of [15], which we do not reproduce here for the sake of brevity.

With these momenta and polarization vectors one can compute the helicity tensors (9) and the associated form factors in the frames B_1 and B_2. Concerning the form factors defined in (16) one has the following. The $\mathcal{C}_i(\lambda_i = \pm 1)$ and $\mathcal{S}_i(\lambda_i = \pm 1)$ are identical to those in the unitary gauge. The $\mathcal{S}_i(\lambda_i = 0)$ are zero because the longitudinal polarization vectors are real vectors. Thus one has to compute only those differential luminosities $\mathcal{J}_{\rm pol}^{\rm axial}$ defined by (25) with $\mathcal{L}_{\rm pol} \to \mathcal{L}_{\rm pol}^{\rm axial}$ where the label "pol" contains at least one index L. We obtain

$$
\mathcal{J}_{\rm LL}^{\rm axial} = c_{\rm LL}\frac{h_1^2 F}{4u^4 k_1^2}\left(1 - \frac{4(u-\nu)^2}{\kappa^2}\right), \tag{B3}
$$

$$
\mathcal{J}_{\rm LT}^{\rm axial} = c_{\rm LT}\frac{-h_1^2 F}{4u^4 k_1^2}\left(1 + \frac{4(u-\nu)^2}{\kappa^2}\right), \tag{B4}
$$

$$
\mathcal{J}_{\rm L\overline{T}}^{\rm axial} = (-1)^{r_2} c_{\rm L\overline{T}}\frac{h_1^2 F}{u^4 k_1^2}\frac{4(\nu-u)}{\kappa}, \tag{B5}
$$

where

$$
\begin{aligned}
F = {} & 4u^2\nu^2 s(s-u) + (k_1^2 k_2^2)^2(u^2 - 6us + 6s^2)\\
& + k_1^2 k_2^2 u(u^3 - 12\nu s^2 - 2u^2(\nu + s) + 2us(6\nu + s)),
\end{aligned}
\tag{B6}
$$

and the couplings $c_{\rm pol}$ are defined in (A13).

Moreover, we find that

$$
\mathcal{J}_{\rm TL}^{\rm axial} = \mathcal{J}_{\rm TL}, \mathcal{J}_{\overline{\rm T}{\rm L}}^{\rm axial} = \mathcal{J}_{\overline{\rm T}{\rm L}}. \tag{B7}
$$

The integrands of these differential luminosities involves the form factor $\mathcal{C}_2(\lambda_2 = 0)$ that happens to be identical in the axial and unitary gauge. Notice, however, that the associated luminosities $\mathbf{L}_{\rm pol}^{\rm axial}(x)$ differ from those in the unitary gauge because in the axial gauge the factors (21) are not taken into account.

[1] G. Aad *et al.* (ATLAS Collaboration), Observation of a new particle in the search for the standard model Higgs boson with the ATLAS detector at the LHC, Phys. Lett. B **716**, 1 (2012).

[2] S. Chatrchyan *et al.* (CMS Collaboration), Observation of a new boson at a mass of 125 GeV with the CMS experiment at the LHC, Phys. Lett. B **716**, 30 (2012).

[3] M. S. Chanowitz and M. K. Gaillard, The TeV physics of strongly interacting W's and Z's, Nucl. Phys. **B261**, 379 (1985).

[4] J. Bagger, V. D. Barger, K. m. Cheung, J. F. Gunion, T. Han, G. A. Ladinsky, R. Rosenfeld, and C.-P. Yuan, CERN LHC analysis of the strongly interacting WW system: Gold plated modes, Phys. Rev. D **52**, 3878 (1995).

[5] C. Englert, B. Jager, M. Worek, and D. Zeppenfeld, Observing strongly interacting vector boson systems at the CERN Large Hadron Collider, Phys. Rev. D **80**, 035027 (2009).

[6] K. Doroba, J. Kalinowski, J. Kuczmarski, S. Pokorski, J. Rosiek, M. Szleper, and S. Tkaczyk, The $W_L W_L$ scattering at the LHC: Improving the selection criteria, Phys. Rev. D **86**, 036011 (2012).

[7] R. N. Cahn and S. Dawson, Production of very massive Higgs bosons, Phys. Lett. B **136**, 196 (1984); Instability of flat spacetime in semiclassical gravity, Phys. Lett. B **138**, 464 (1984).

[8] S. Dawson, The effective W approximation, Nucl. Phys. **B249**, 42 (1985).

[9] G. L. Kane, W. W. Repko, and W. B. Rolnick, The effective $W^{\pm}$, Z^0 approximation for high-energy collisions, Phys. Lett. B **148**, 367 (1984).

[10] S. Dawson, Radiative corrections to the effective W approximation, Phys. Lett. B **217**, 347 (1989).

[11] Z. Kunszt and D. E. Soper, On the validity of the effective W approximation, Nucl. Phys. **B296**, 253 (1988).

[12] P. Borel, R. Franceschini, R. Rattazzi, and A. Wulzer, Probing the scattering of equivalent electroweak bosons, J. High Energy Phys. 06 (2012) 122.

[13] R. Kleiss and W. J. Stirling, Anomalous high-energy behavior in boson fusion, Phys. Lett. B **182**, 75 (1986).

[14] P. W. Johnson, F. I. Olness, and W. K. Tung, The effective vector boson method for high-energy collisions, Phys. Rev. D **36**, 291 (1987).

[15] I. Kuss and H. Spiesberger, Luminosities for vector boson-vector boson scattering at high-energy colliders, Phys. Rev. D **53**, 6078 (1996).
[16] S. S. D. Willenbrock and D. A. Dicus, Production of heavy quarks from W gluon fusion, Phys. Rev. D **34**, 155 (1986).
[17] S. Dawson and S. S. D. Willenbrock, Heavy fermion production in the effective W approximation, Nucl. Phys. **B284**, 449 (1987).
[18] R. P. Kauffman, Production of top quarks via vector boson fusion in e^+e^- collisions, Phys. Rev. D **41**, 3343 (1990).
[19] F. Larios, T. M. P. Tait, and C. P. Yuan, Anomalous $W^+W^-t\bar{t}$ couplings at the e^+e^- linear collider, Phys. Rev. D **57**, 3106 (1998).
[20] J. F. Gunion, J. Kalinowski, and A. Tofighi-Niaki, Exact Calculation of $ff \to ffWW$ for the Charged Current Sector and Comparison With the Effective-W Approximation, Phys. Rev. Lett. **57**, 2351 (1986).
[21] E. Accomando, A. Ballestrero, A. Belhouari, and E. Maina, Isolating vector boson scattering at the LHC: Gauge cancellations and the equivalent vector boson approximation vs complete calculations, Phys. Rev. D **74**, 073010 (2006).
[22] E. Accomando, A. Denner, and S. Pozzorini, Logarithmic electroweak corrections to $e^+e^- \to V_e\bar{\nu}_e W^+W^-$, J. High Energy Phys. 03 (2007) 078.
[23] N. Bouayed and F. Boudjema, One-loop electroweak and QCD corrections to vector boson scattering into top pairs and application to ILC, Phys. Rev. D **77**, 013004 (2008).
[24] A. Alboteanu, W. Kilian, and J. Reuter, Resonances and unitarity in weak boson scattering at the LHC, J. High Energy Phys. 11 (2008) 010.
[25] W. Kilian, T. Ohl, and J. Reuter, WHIZARD: Simulating multi-particle processes at LHC and ILC, Eur. Phys. J. C **71**, 1742 (2011).
[26] J. Alwall, R. Frederix, S. Frixione, V. Hirschi, F. Maltoni, O. Mattelaer, H.-S. Shao, T. Stelzer, P. Torrielli, and M. Zaro, The automated computation of tree-level and next-to-leading order differential cross sections, and their matching to parton shower simulations, J. High Energy Phys. 07 (2014) 079.
[27] K. Arnold *et al.*, VBFNLO: A parton level Monte Carlo for processes with electroweak bosons–Manual for Version 2.7.0, arXiv:1107.4038.
[28] J. Baglio *et al.*, Release Note–VBFNLO 2.7.0, arXiv: 1404.3940.
[29] J. Brehmer, J. Jaeckel, and T. Plehn, Polarized WW scattering on the Higgs pole, Phys. Rev. D **90**, 054023 (2014).
[30] I. Kuss, Improved effective vector boson approximation for hadron hadron collisions, Phys. Rev. D **55**, 7165 (1997).
[31] C. Dams and R. Kleiss, The electroweak standard model in the axial gauge, Eur. Phys. J. C **34**, 419 (2004).